

Metal MEMS Membrane Based Electric Field Sensor

E.Tahmasebian¹, C.Shafai, Tao Chen

Department of Electrical and Computer Engineering

University of Manitoba, Winnipeg, MB, Canada R3T 2N2, ¹tahmasee@cc.umanitoba.ca

Abstract: A MEMS based electrostatic field sensor is presented which uses capacitive interrogation of an electrostatic force deflected microstructure. The deflection of the sensor is calculated both by simulation and theoretical model and it has been shown that the results of the simulations have acceptable values compared to the theoretical ones. Simulation models have also been designed to solve the resonating issue of the membrane for measuring the AC electric fields. It has been shown that by adding perforations to the surface of the membrane, it is possible to reduce the mass of membrane and still have similar electrostatic force on the membrane. Therefore, it is possible to reduce the damping due to air resistance in membrane movement when measuring AC fields.

Keywords: electric field measurement, electric field sensor, micro-electromechanical systems, metal MEMS

1. Introduction

Measuring the electric field under the HVDC transmission lines is important for power utilities, as well as atmospheric analysis. Field mills are conventional devices for measuring the DC electric fields, however do to their high power consumption, there is an interest for using low power devices such as micromachined electric field mills (MEFMs) instead. Several groups have researched different type of MEFMs before [1,2]. In [3], our group developed an electrostatic force deflected membrane based sensor. Roncin et al. implemented a laser deflection measurement system (Figure 1) for measuring the deflection of the membrane. The problem with the laser system was large power consumption, therefore a subsequent version of the sensor was designed to use capacitive interrogation of the deflected membrane position (Figure 2) [4]. The metalized membrane will be deflected to the voltage source due to the electrostatic force and the deflection will result in the change of the capacitance between membrane and the electrode beneath.

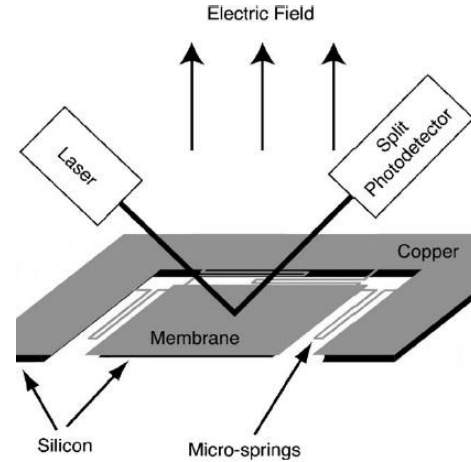


Figure 1: Laser deflection measurement system.

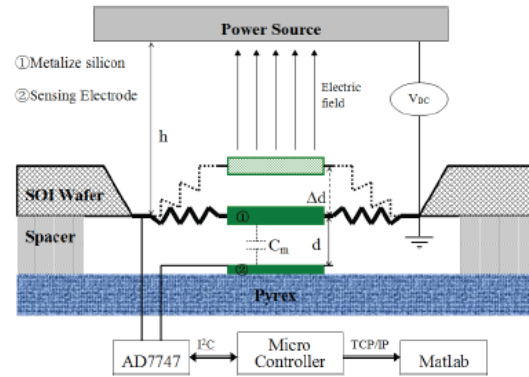


Figure 2: Capacitive interrogation system for measurement of membrane deflection.

The change in the capacitance C_m is measured with a capacitance to digital converter chip and sent to the computer for post processing. The first generation of the sensor has been successfully fabricated in an SOI wafer process, and tested. However, the SOI wafers are expensive, therefore, in order to reduce the cost of fabrication electroplating of the low stress thick metals instead of SOI wafer could be an alternative. The other benefits of electroplated thick films (copper or nickel) are their robustness. Therefore, our group is designing the next generation of our sensors with electroplated copper. The first step for that is simulation to check the spring constant and range of the

membrane deflection under applied electric fields. Here we are presenting the sensor model and the set up which are simulated by COMSOL. In addition, in the present work simulations have been done to explore the damping problem for membrane resonance while the sensor is used under AC electric fields.

2. Sensor Design and Operation Principle

2.1 Design

The sensor consists of a membrane that is suspended by the four springs (Figure 3). The membrane measures 1 mm x 1 mm and the springs are 30 μm wide with width of 470 μm . The whole membrane structure and springs are made of copper, and the ends of the springs are fixed by connecting to a copper substrate. Two sets of simulations have been done with 5 μm and 10 μm as the thickness of the membrane and springs. These thicknesses are chosen to have a robust and flexible membrane at the same time.

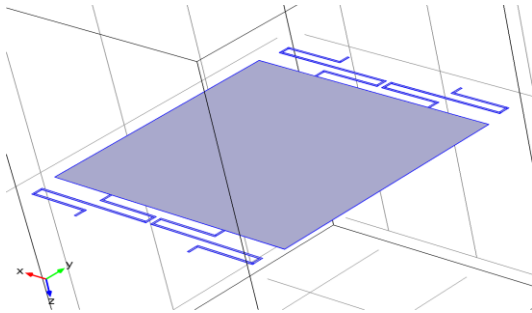


Figure 3: Simulated sensor structure.

2.2 Operation Principle

The incident electric field will pull the membrane toward the voltage source, this electrostatic force is calculated by [5]:

$$F_e = \frac{1}{2} \frac{\epsilon A}{h^2} V_{DC}^2 = \frac{1}{2} \epsilon A E^2 \quad (1)$$

where A is the surface area of the membrane, V is the voltage of the voltage source, ϵ is the permittivity of air, E is the of the electric field and h is the of the distance between membrane and voltage source. The restoring force on the springs is given by:

$$F_s = k\Delta d \quad (2)$$

where k is the spring constant (total of the four micro-springs supporting the membrane). The relationship between the incident electric field that causes membrane motion, and the variation of the capacitance measured by the position sensing electrode, derived by Chen et al. [6].

$$\Delta C = \frac{C_{m\text{ initial}}^2}{\frac{2k}{E^2} + C_{m\text{ initial}}} \quad (3)$$

where $\Delta C = C_{m\text{ initial}} - C_{m\text{ final}}$.

3. Use of COMSOL Multiphysics

By using symmetry, only a quarter of the sensor has been simulated in order to save time and memory. The electromechanics module is used for defining mechanical and electrical conditions of the model. A box of air is surrounding the sensor in the model and an electrical potential is applied to the topside while the springs, membrane and bottom side of the box are electrically grounded. The end of each spring is defined as a fixed constraint.

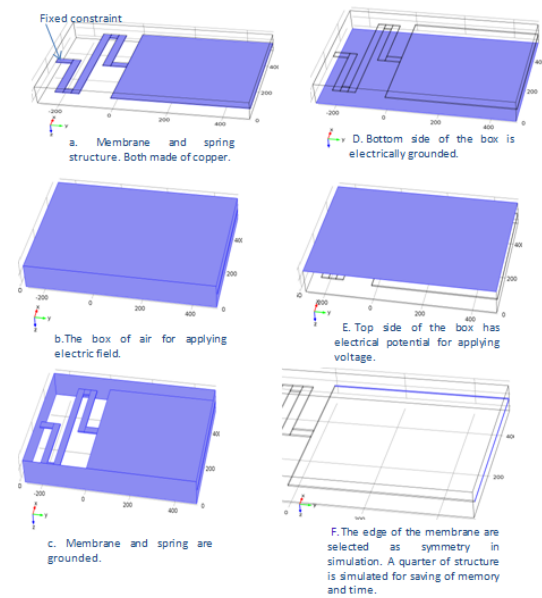


Figure 4: Electrical and mechanical applied conditions.

4. Simulations and Results

4.1 Membrane deflection under DC field

The previous version of the sensor [6] was a silicon based membrane which was 5 μm thick

and had 200 nm sputtered copper surface coating. Since the membrane of this paper will be made entirely from copper, the first set of simulations should be done to check the range of the deflection of membrane, in order to see whether the new design have enough deflection range to be sensed with the capacitance interrogation system. Second, the model should determine if results are agree with theoretical expected values based on equation (2). Due to the limitation in fabrication process and need for enough strength in the membrane, copper thicknesses between 2 - 10 μm are investigated. The results for the deflection of the membrane for different electric fields for thickness of 5 μm and 10 μm are shown in Table 1. In Table 2 the expected deflection values based on the theoretical formula are shown. We can see that the deflections for both theoretical and simulations agree and the range of the deflection is in the same order. In addition, the range of the deflection of membrane is large enough to be detected by our capacitance to digital convertor chip (AD7747) [7].

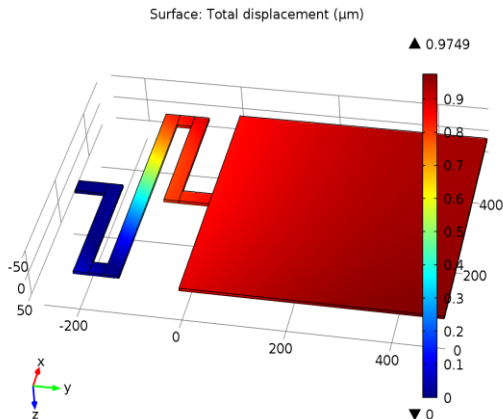


Figure 5: The simulation results for the deflection of the membrane in presence of 50 kV/m electric field.

Table 1: Simulation results for membrane sensor deflection vs. incident electric field.

| Electric Field | 10 (kV/m) | 50 (kV/m) | 100 (kV/m) | 500 (kV/m) | 1000 (kV/m) |
|--|-----------|-----------|------------|------------|-------------|
| 5 μm thick copper membrane | 3.77e-4 | 9.33e-3 | 0.0374 | 0.975 | 4.55 |
| 10 μm thick copper membrane | 5.98e-5 | 1.49e-3 | 3.98e-3 | 0.151 | 0.616 |

Table 2: Theoretical expected values for membrane sensor deflection.

| Electric Field (kV/m) | 10 (kV/m) | 50 (kV/m) | 100 (kV/m) | 500 (kV/m) | 1000 (kV/m) |
|--|-----------|-----------|------------|------------|-------------|
| 5 μm thick copper membrane | 4.23e-4 | 10.6e-3 | 0.0422 | 0.106 | 4.22 |
| 10 μm thick copper membrane | 6.41e-5 | 1.60e-3 | 6.41e-3 | 0.160 | 0.641 |

4.2 New design for solving the damping Under AC Field

This sensor system can also be implemented for the measurement of AC electric fields. The main difference between measuring the DC and AC electric fields is the motion of the membrane. Under the DC field, the membrane will be deflected to a steady state, however in the AC case the membrane vibrates. Imagine the case that we want to measure the amplitude of an AC electric field that has the same value of a DC electric field. In this case, and assuming no air drag and mass effects, the highest deflection of the membrane should be the same as the deflection of the membrane in the steady state for measuring DC signals. This is only possible when the membrane's resonance is higher than the AC field frequency, and if air drag effect is minimized. For studying this situation a new model for the sensor is described below.

4.2.1 Membrane with holes

In the new design, holes have been added to the surface of the membrane. Since we want to do the capacitance measurement, it is important understand if the holes will affect the electrostatic force on the membrane from the incident field. This can be explored by determining if any incident field causes a charge build-up on the capacitive interrogating electrode below the perforated membrane, since any charge on the underlying electrode would be a reduction in membrane charge, and so force on the membrane. To simulate this a fixed grounded copper electrode has been added to the model beneath the membrane (Figure 6). It has the same size of the membrane with same thickness. The model is used to first explore up to what size of holes the charge on the lower electrode would be negligible. Simulations were run for nine

rectangular holes of the same size. The results are shown in Table 3.

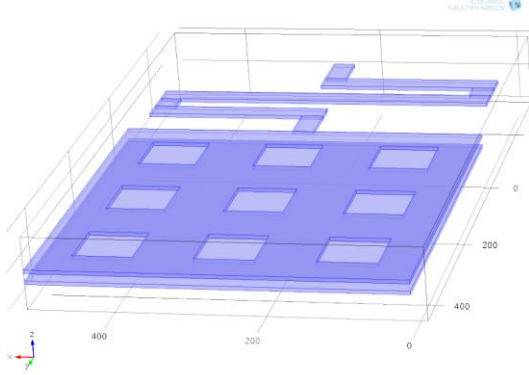


Figure 6: Sensor structure for AC measurement.

In the Table 3, Q1 stands for the charge on the total surface of the membrane and the Q2 stands for the charge on the surface of the lower electrode. It can be seen in Table 3 that for the holes with size less than $50 \times 50 \mu\text{m}$, the value of Q2 compared to Q1 is less than 5%, and the reduction in Q1 is below 5%.

Table 3: Total charge at the surface of membrane and lower electrode. The electric field, thickness of the membrane and lower electrode spacing were 10 kV/m, $5 \mu\text{m}$, $5 \mu\text{m}$ respectively.

| Hole size | Q1: Membrane charge (C) | Q2: Underlying electrode charge (C) |
|---------------------|-------------------------|-------------------------------------|
| No holes | -5.59e-14 | -5.64e-16 |
| 10x10 μm | -5.57e-14 | -5.62e-16 |
| 20x20 μm | -5.51e-14 | -6.29e-16 |
| 30x30 μm | -5.44e-14 | -8.36e-16 |
| 40x40 μm | -5.36e-14 | -1.10e-15 |
| 50x50 μm | -5.32e-14 | -1.41e-14 |
| 60x60 μm | -4.99e-14 | -2.67e-13 |

A second set of simulations is shown in Table 4, where the membrane is perforated with an array of many holes, confined within a boundary of 50 μm from the edge of the membrane. Three simulations are done, with $20 \times 20 \mu\text{m}$ holes with $20 \mu\text{m}$ spacing, $40 \times 40 \mu\text{m}$ holes with $40 \mu\text{m}$ spacing, and $80 \times 80 \mu\text{m}$ holes with $80 \mu\text{m}$ spacing (Figure 7). The simulations for the three different sizes of the holes are shown in Table 4. As shown in Table 4 with holes up to the 40×40

μm size, Q2 is below 5% from Q1. However, Q1 itself falls considerably compared to the case with no holes in the membrane shown in Table 3. This is due to the considerably larger surface area of holes, compared to the case in Table 3. Further study will need to be done with thicker membranes, and for larger membrane to underlying electrode spacing, to minimize the reduction in charge Q1 on the membrane, due to the presence of holes on the membrane surface.

Table 4: Total charge at the surface of membrane and lower electrode. The electric field, thickness of the membrane and lower electrode spacing were 10 kV/m, $5 \mu\text{m}$, $5 \mu\text{m}$ respectively.

| Hole size | Q1: Membrane charge (C) | Q2: Underlying electrode charge (C) |
|---------------------|-------------------------|-------------------------------------|
| 20x20 μm | -4.84e-14 | -2.23e-16 |
| 40x40 μm | -4.49e-14 | -3.70e-16 |
| 80x80 μm | -4.00e-14 | -6.22e-15 |

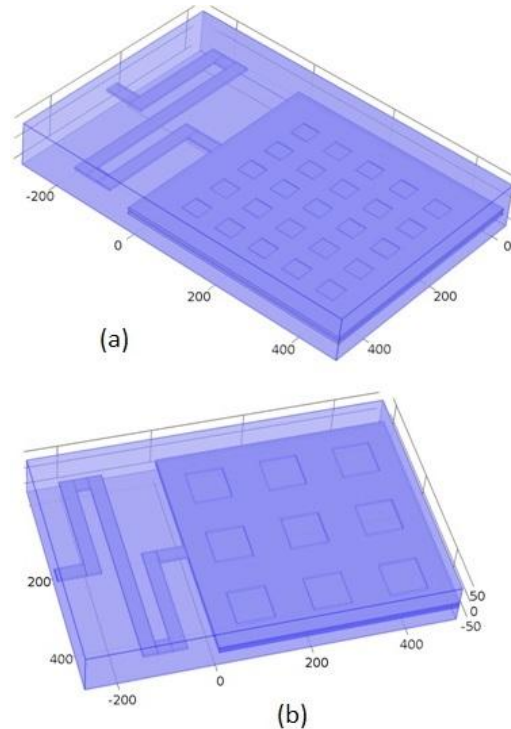


Figure 7: Membrane design with 50% duty cycle holes: (a) 40×40 holes. (b) 80×80 holes.

5. Future Work

The simulated design will be fabricated and tested to explore its operation parameters. For the AC measurement, the structure of the sensor is not still optimized. Several factors such as spacing between the holes and gap between the membrane and lower electrode should be studied to find the minimum mass of the membrane with the highest charge on the surface of the membrane. As well, the effect of the air drag on the sensor motion for incident AC electric fields needs to be explored as a function of perforation geometry.

6. Conclusions

A new design has been shown for the membrane based electric field sensor. For DC electric field measurement simulations, the electrostatic force applied to the membrane deflects the membrane vertically towards the field. The deflection of the membrane has been calculated from both theory and simulation by COMSOL. Comparing the simulation results and the expected theoretical values shows that the model is working properly and this design potentially is a proper design for the sensor. In addition, the range of the deflection of membrane is large enough to be detected by our capacitance to digital convertor (AD7747). Simulations were done to explore perforated membranes for operation in the presence of AC fields. Holes added to the surface of the membrane reduce its mass and allow for air flow through the membrane. However, larger holes result in reduced the electrostatic force on the membrane, reducing sensor sensitivity.

Acknowledgements

This research was funded by the Natural Sciences and Engineering Research Council (NSERC) of Canada, and Manitoba Hydro Inc. of (Winnipeg, Canada).

References

1. Gayan Wijeweera, Behraad Bahreyni, Cyrus Shafai, and Athula Rajapakse, "Micromachined electric-field sensor to measure AC and DC fields in power systems", *IEEE Trans. Power Delivery*, vol. 24, pp. 988-995 July 2009.
2. Takeshi Kobayashi, Syoji Oyama, Masaharu Takahashi, Ryutaro Maeda, and Toshihiro Itoh, "Microelectromechanical system-based electrostatic field sensor", *Japanese Journal of Applied Physics*, vol. 47, pp. 7533-7536, 2008.
3. Andrew Roncin, Cyrus Shafai, and D.R. Swatek, "Electric field sensor using electrostatic force deflection of a micro-spring supported membrane", *Sensors and Actuators A*, vol. 123-124, pp. 179-184, Sept. 2005.
4. Tao Chen, Ehsan Tahmasebian, and Cyrus Shafai, "MEM electric Field sensor using force deflection mechanism", *Manitoba Materials Conference*, Spring 2013.
5. Ki Bang Lee, "Principles of Microelectromechanical Systems", A John Wiley & Sons, Inc., pp. 513-519, 2011.
6. Tao Chen and Cyrus Shafai, "MEM Electric Field Sensor using Force Deflection with Capacitance Interrogation," 2013 IEEE Power & Engineering Society (PES) General Meeting, Vancouver, July 21-25, 2013.
7. 24-Bit Capacitance-to-Digital Converter with Temperature Sensor (AD7747 datasheet), Analog Devices, 2007 [Online].